

Detection of Fleeting Amine Radical Cations and Elucidation of Chain Processes in Visible-Light-Mediated [3 + 2] Annulation by Online **Mass Spectrometric Techniques**

Yi Cai, †,§ Jiang Wang, ‡,§ Yuexiang Zhang, †,§ Zhi Li,† David Hu,† Nan Zheng,*,‡ and Hao Chen*,†

Supporting Information

ABSTRACT: Visible-light-mediated photoredox reactions have recently emerged as a powerful means for organic synthesis and thus have generated significant interest from the organic chemistry community. Although the mechanisms of these reactions have been probed by a number of techniques such as NMR, fluorescence quenching, and laser flash photolysis and various degrees of success has been achieved, mechanistic ambiguity still exists (for instance, the involvement of the chain mechanism is still under debate) because of the lack of structural information about the proposed and short-lived intermediates. Herein, we present the detection of transient amine radical cations involved in the intermolecular [3 + 2] annulation reaction of N-cyclopropylaniline (CPA, 1) and styrene 2 by electrospray ionization mass spectrometry (ESI-MS) in combination with online laser irradiation of the reaction mixture. In particular, the reactive CPA radical cation 1+0, the reduced photocatalyst

 $Ru(I)(bpz)_3^+$, and the [3+2] annulation product radical cation $3^{+\bullet}$ are all successfully detected and confirmed by high-resolution MS. More importantly, the post-irradiation reaction with an additional substrate, isotope-labeled CPA, following photolysis of 1, 2, and Ru catalyst provides strong evidence to support the chain mechanism in the [3+2] annulation reaction. Furthermore, the key step of the proposed chain reaction, the oxidation of CPA 1 to amine radical cation 1^{+•} by product radical cation 3^{+•} (generated using online electrochemical oxidation of 3), is successfully established. Additionally, the coupling of ESI-MS with online laser irradiation has been successfully applied to probe the photostability of photocatalysts.

■ INTRODUCTION

Photoredox catalysis has recently become a topic of intense study in the field of organic chemistry. The heightened interest in this topic is likely attributed to photoredox catalysis' versatility in generating radicals using light under mild conditions, a specific mode of activation that is different from how radicals are produced under non-photo conditions.² As such, it provides a means to explore radical chemistry that is complementary to that under non-photo conditions. Moreover, photoredox catalysis' ability to merge with other types of catalysis to form dual catalysis further expands its utility far beyond the scope of traditional radical chemistry.³

In contrast to the furious activity in method development for photoredox catalysis, mechanistic studies have been rather scarce.4 In the published, limited results, there exists controversy, such as whether photoredox reactions involve chain processes. This is an important mechanistic question in method development as different approaches are required to optimize the two processes separately. Light/dark experiments have been often used to differentiate them. 4-6 However, there remains the ambiguity of interpreting the results of light/dark experiments; the chain mechanism was established by other methods, whereas light/dark experiments disproved its involvement. 6a,b Quantum yield measurements are, in principle, a more general and sensitive method to differentiate the two competing processes. However, a wide range of quantum yields from 1.3 to 77 across several types of photoredox reactions have been reported, 4g-i,6b which makes distinction of the two processes more difficult, particularly for those with quantum yields close to 1. Clearly, there is a strong need for the development of new tools that allow for explicit elucidation of photoredox reaction mechanisms including identification of both the photoredox process and the chain mechanism.

Photoredox reactions pose a significant challenge to chemists who are interested in studying their mechanisms. They are typically fast and reversible, and the intermediates are shortlived. A variety of techniques such as NMR, EPR, fluorescence quenching, quantum yield measurement, and laser flash photolysis have been employed to study photoredox

Received: June 17, 2017 Published: August 8, 2017

12259

[†]Department of Chemistry and Biochemistry, Center of Intelligent Chemical Instrumentation, Edison Biotechnology Institute, Ohio University, Athens, Ohio 45701, United States

[‡]Department of Chemistry and Biochemistry, University of Arkansas, Fayetteville, Arkansas 72701, United States

reactions. 4,6 However, these spectroscopic methods usually lack structural information on the transient intermediates. Mass spectrometry (MS) has become a powerful technique for detecting and characterizing short-lived reaction intermediates as well as studying reaction mechanisms since the advent of soft ionization methods such as electrospray ionization (ESI)⁷ and desorption electrospray ionization.8 The inherent high sensitivity and rich mass information provided by MS measurements distinguish it from other commonly used methods. Moreover, in comparison to traditional spectroscopic approaches, it is a general technique and does not need chromophore-carrying substrates for investigating reaction mechanisms. However, the probed species such as substrates, catalysts, intermediates, or products must carry a charge, and sometimes the detection can suffer from ion suppression effects due to the matrix effect.

We recently developed an intermolecular [3 + 2] annulation of N-cyclopropylanilines with alkenes by photoredox catalysis (Scheme 1). This reaction displays some excellent features for

Scheme 1. Intermolecular [3 + 2] Annulation of N-Cyclopropylaniline 1 and Styrene 2 Catalyzed by $Ru(II)(bpz)_3(PF_6)_2$

a synthetic method such as broad functional group compatibility, 100% atom economy, and an overall redox-neutral process. The scope of this reaction was later expanded to include various π bonds. These results have opened new avenues for the use of aniline-substituted cyclopropanes as synthetic building blocks. 11 Mechanistically, these methods are all believed to proceed through ring opening of the amine radical cations of N-cyclopropylanilines. This process has been previously studied by EPR^{12a} and electrochemical methods. ^{12b} However, it has not been studied in the context of a complete catalytic cycle, which is more relevant to our efforts in expanding this reaction class to include other types of aminesubstituted carbocycles. Therefore, we were eager to study the complete catalytic cycle of the [3 + 2] annulation reaction.

Herein, we designed a series of online ESI-MS apparatus (Figure 1) that allowed the direct detection of the short-lived intermediates including the substrate radical cation $1^{+\bullet}$ and the product radical cation $3^{+\bullet}$ from the visible-light-mediated [3 + 2] annulation catalyzed by Ru(II)(bpz)₃(PF₆)₂ (see structures of 1^{+•} and 3^{+•} in Scheme 2). Although MS in combination with online photolysis (e.g., using a lamp or laser to irradiate a reaction mixture prior to MS detection) has been previously reported in literature, 7q,13 this type of setup has been rarely used to study the mechanism of visible-light-triggered photoredox reactions.^{7q} Moreover, none of the reported MS studies provided any conclusive evidence for the chain reaction mechanism involved in photoredox reactions. Our setup not

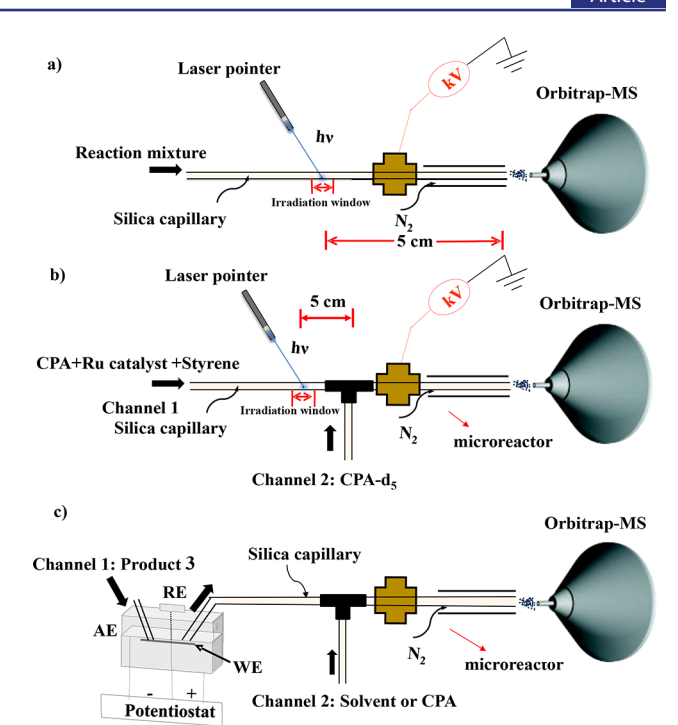


Figure 1. (a) Apparatus showing direct monitoring of the photoredox reaction by online ESI-MS. (b) Apparatus allowing the post-irradiation reaction event to be investigated: a reaction mixture is introduced into the silica capillary, photoexcited by the laser pointer, and then mixed with an isotope-labeled new substrate introduced via channel 2. (c) Apparatus for investigating the reactivity of the radical cation generated via online electrolysis: a thin-layer electrochemical flow cell is connected with an ion source, and a substrate is introduced via channel 2 for testing the key electron transfer step involved in the chain mechanism. AE, RE, and WE represent auxiliary electrode, reference electrode, and working electrode, respectively.

Electrochemical flow cell

only allows for the direct detection of elusive reaction intermediates via online photolysis using a laser pointer (Figure 1a) but also enables it to be coupled with an online microreactor to study the reactivities of the reaction intermediates. For instance, another reagent such as CPA- d_5 was introduced downstream via a second channel (Figure 1b). In addition, for those intermediates that could not be generated photochemically (e.g., the radical cation of the [3 + 2] annulation product 3+0), electrolysis was employed as an alternative way to generate radical cation 3^{+•}, whose reactivity could then be monitored online by MS (Figure 1c). A combination of electrochemistry with MS has been one of our research focuses and has applications for studying redox chemistry of both small organic molecules and large protein molecules. 8d,14 In this study, using the setup, we obtained unequivocal evidence to support the involvement of the chain processes in the [3 + 2] annulation reaction. Because the setup is flexible and modular, we believe that it can be easily adopted to study other photoredox reactions.

■ RESULTS AND DISCUSSION

Apparatus. A high-resolution Q Exactive Plus hybrid quadrupole-Orbitrap mass spectrometer (Thermo Fisher Scientific, San Jose, CA) was used in this study. As shown in Figure 1a, to probe reaction intermediates, the commercial ESI ion source was removed to accommodate an in-house-made

ESI source. A piece of fused Silica capillary (100 μ m i.d., 198 μ m o.d.) was used to deliver the reaction mixture solution for online photolysis and online ESI-MS analysis (Figure 1a). An irradiation window on the silica capillary (1 cm wide), located ca. 5 cm upstream from the ESI emitter tip, was made by burning away the organic capillary coating with flame. A laser pointer (403 nm, 50 mW, LaserPointerPro, HK) was employed as a light source to irradiate the reaction solution in the capillary to trigger the photoredox reaction as the solution flowed by the irradiation window. The laser pointer was held about 5 cm away from the irradiation window. A high voltage +5 kV was applied to ionize the reaction mixture, with the assistance of 170 psi N₂ nebulization gas. The reaction solutions were all rigorously degassed with argon before irradiation. The flow rate for infusing the reaction mixture solution through the silica capillary was 100 μ L/min. The transportation time for the reaction mixture flowing from the irradiation window to the ESI emitter tip was about 236 ms (dead volume = 0.393 μ L, flow rate = 100 μ L/min).

To investigate the chain propagation process, the original MS setup described in Figure 1a was modified to perform a sequential reaction experiment (Figure 1b), in which a reaction mixture (e.g., a mixture of N-cyclopropylaniline (CPA) 1, styrene 2, and $Ru(II)(bpz)_3(PF_6)_2$ 4) was introduced into the silica capillary via channel 1 (50 μ L/min), photoexcited by the laser pointer, and then mixed with an isotope-labeled new substrate (introduced via channel 2, 50 μ L/min). Upon mixing, the added substrate reacted with the photoexcited reaction mixture in the downstream capillary serving as a microreactor prior to MS detection. Because the isotope-labeled substrate was added after the photolysis of the reaction mixture, positive identification of the product derived from the added isotopelabeled substrate could be used as evidence to support the chain propagation process. The inherent high sensitivity of MS enabled detection of the product in minute amounts, which made this apparatus far more sensitive than dark/light experiments.

Alternatively, photolysis could be replaced by electrolysis to generate the amine radical cation of product 3. As shown in Figure 1c, an electrochemical flow cell with a magic diamond electrode (details shown in the text below) was used in our experiment. Amine radical cation 3^{+•} was then mixed with CPA 1 introduced via channel 2 to examine its reactivity by online MS monitoring. In this case, high voltage was not applied to the ESI source to avoid a voltage conflict issue between the electrochemical cell and the ion source. Photos of all of the experimental setups mentioned above are included in the Supporting Information (Figure S1).

Detection of Amine Radical Cations. CPA 1 and styrene 2 were chosen as the model substrates (Scheme 1) to investigate the intermolecular [3 + 2] annulation catalyzed by Ru(II)(bpz)₃(PF₆)₂ 4 using the ESI-MS setup with online photolysis shown in Figure 1a. We selected this pair of substrates because both were extensively studied in the initial development of the annulation reaction. ^{9,10}

As previously proposed (Scheme 2),9 upon irradiation, $Ru(II)(bpz)_3^{2+}$ is promoted to the photoexcited triplet state $Ru(II)^*(bpz)_3^{2+}$, which oxidizes CPA 1 to amine radical cation $1^{+\bullet}$ with the concomitant formation of $Ru(I)(bpz)_3^+$. Amine radical cation 1+0 subsequently undergoes ring opening and is then added intermolecularly to styrene 2 to produce the [3 + 2]annulation product radical cation 3^{+•}. Reduction of 3^{+•} by Ru(bpz)₃⁺ completes the catalytic cycle. Alternatively, a chain

Scheme 2. Proposed Mechanism for the [3 + 2] Annulation Reaction of N-Cyclopropylaniline 1 and Styrene 2 Catalyzed by $Ru(II)(bpz)_3(PF_6)_2$

mechanism involves the oxidation of CPA 1 by amine radical cation $3^{+\bullet}$ to a new radical cation $1^{+\bullet}$ while $3^{+\bullet}$ is reduced to product 3, allowing closure of the catalytic cycle.

To probe the above reaction mechanism, online irradiation and detection experiments using the aforementioned apparatus (Figure 1a) were first carried out. In this experiment, we started with the examination of the reaction between Ru(II)- $(bpz)_3(PF_6)_2$ 4 and CPA 1 under the photolysis conditions. A mixture of $[Ru(II)(bpz)_3](PF_6)_2$ 4 (0.0004 mmol, 100 μ M) and CPA 1 (0.02 mmol, 5 mM) in 4 mL of CH₃NO₂ was infused at a flow rate of 100 μ L/min through the silica capillary for ESI-MS detection after argon degassing. An ESI-MS spectrum was acquired without irradiating the reaction solution flowing through the capillary with a laser (Figure 2a). Ions of m/z 134 (measured m/z, 134.0966; theoretical m/z, 134.0964; error, +1.5 ppm) and m/z 288 (measured m/z, 288.0408; theoretical m/z, 288.0405; error, -1.0 ppm) were detected, corresponding to the protonated CPA [1 + H]+ and $Ru(II)(bpz)_3^{2+}$, respectively. We noticed that there was a small peak for $\mathbf{1}^{+\bullet}$ (measured m/z, 133.0888; theoretical m/z, 133.0886; error, +1.5 ppm; Figure 2a, inset) with an intensity of 1.69×10^6 (arbitrary units). We attributed the formation of $1^{+\bullet}$ to in-source oxidation of 1 during the ESI ionization process. 15 as it was still observed in the absence of Ru catalyst 4. Furthermore, the reduced Ru(I) species was not observed.

Next, when the laser pointer was turned on to irradiate the mixture in the capillary through the irradiation window, the intensity of the 1^{+•} peak increased 17-fold (Figure 2b, inset), which was ascribed to the photo-oxidation of 1. Amine radical cation $\mathbf{1}^{+\bullet}$ could undergo ring opening to furnish the distonic radical cation. However, ESI-MS cannot differentiate the two species because they have the same mass. Additionally, a reduced Ru catalyst peak of $Ru(I)(bpz)_3^+$ at m/z 576 (measured m/z, 576.0815; theoretical m/z, 576.0815; error, 0.0 ppm) was also detected. The inset in Figure 2b clearly shows the zoomed-in spectrum of Ru(I)(bpz)₃⁺ at m/z 576 (in black), which matches well with its theoretical isotopic peak distribution (in red). This experimental result supports the photooxidation of CPA 1 by photoexcited Ru(II)*(bpz)₃^{2+,2d} A control study in which CPA 1 from the reaction mixture was replaced by styrene 2 (Figure S2) showed no formation of $Ru(I)(bpz)_3^+$, excluding the possibility of a redox reaction between $Ru(II)^*(bpz)_3^{2+}$ and styrene 2. Both results were consistent with Stern-Volmer studies in which CPA 1 was

Journal of the American Chemical Society

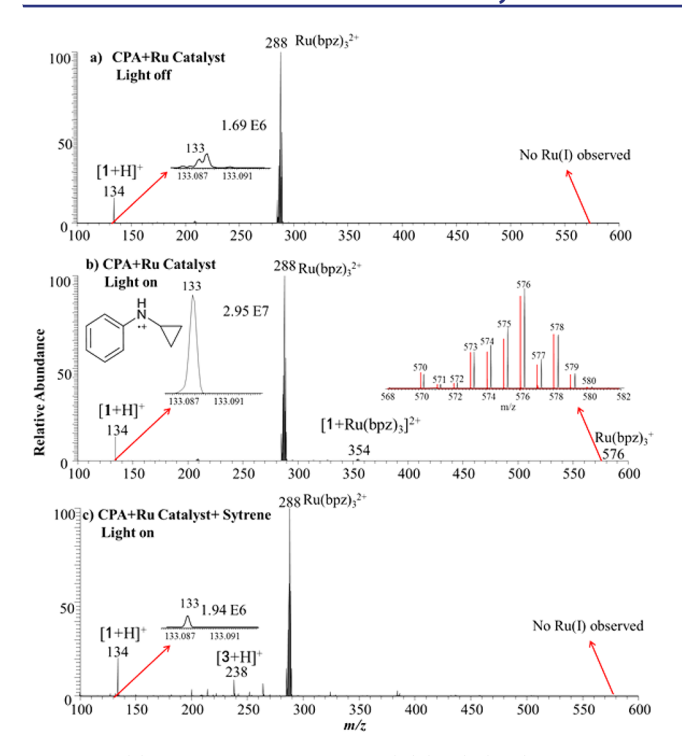


Figure 2. (a) ESI-MS spectrum of $Ru(II)(bpz)_3(PF_6)_2$ and CPA in CH_3NO_2 acquired without light irradiation. (b) ESI-MS spectrum of $Ru(II)(bpz)_3(PF_6)_2$ and CPA in CH_3NO_2 with light irradiation. (c) ESI-MS spectrum of $Ru(II)(bpz)_3(PF_6)_2$, CPA, and styrene in CH_3NO_2 with light irradiation.

shown to be an effective quencher for $Ru(II)*(bpz)_3^{2+}$ but styrene 2 was not (Figures S14 and S16).

Next, we monitored the [3 + 2] annulation of CPA 1 and styrene 2 in CH₃NO₂ with Ru catalyst 4 using ESI-MS. A degassed mixture of $[Ru(bpz)_3](PF_6)_2$ 4 (0.0004 mmol, 100 μ M), CPA 1 (0.02 mmol, 5 mM), and styrene 2 (0.4 mmol, 0.1 M) in 4 mL of CH₃NO₂ was irradiated inside the capillary by the laser pointer, and the reaction was monitored online by ESI-MS. Under irradiation, the protonated [3 + 2] annulation product $[3 + H]^+$ (m/z 238) (measured m/z, 238.1593; theoretical m/z, 238.1590; error, +1.2 ppm) was clearly observed (Figure 2c). Upon collision-induced dissociation (CID), ion m/z 238 gave rise to a fragment ion of m/z 145 by loss of C₆H₅NH₂ (Figure S3a), consistent with its assigned structure. Furthermore, the CID behavior of this ion was identical to that of the protonated product at m/z 238 generated from ESI of the authentic product compound 3 (Figure S3b), reinforcing the ion assignment. Although a small peak for CPA radical cation 1^{+•} was seen (Figure 2c, inset; its intensity is similar to that seen in Figure 2a), it was again probably due to in-source ESI oxidation of unreacted CPA 1. There were a few unassigned peaks in Figure 2c, whose suggested chemical formulas are included in Table S1. Surprisingly, the product radical cation 3^{+•} was not observed in the acquired MS spectrum under these conditions, which will be discussed further subsequently. Notably, $Ru(I)(bpz)_3^+$ $(m/z)_3^+$ 576) could not been observed in Figure 2c, presumably because it was consumed in the annulation reaction. This data supports a photoredox process in which Ru(I)(bpz)₃⁺ reduces the product radical cation 3^{+•} to complete the catalytic cycle (Scheme 2). The two processes, the photoredox process and the chain mechanism, likely compete against each other and are intertwined throughout the reaction.

We encountered difficulties in detecting the product radical cation $3^{+\bullet}$ during our studies of the online photolysis of CPA 1 and styrene 2 in the presence of Ru catalyst 4 (Figure 2c). We surmised that a higher concentration of CPA 1 would result in a faster chain reaction between the product radical cation $3^{+\bullet}$ and CPA 1 and thus would shorten the lifetime of $3^{+\bullet}$. Alternatively, a higher concentration of CPA 1 could lead to a higher concentration of Ru(I) via reduction of the excited Ru(II) complex, which could also shorten the lifetime of $3^{+\bullet}$ via a photoredox process (Scheme 2).

To test this hypothesis and observe radical cation $3^{+\bullet}$, we performed an ESI-MS monitoring experiment by lowering the concentration of CPA 1 from 5 mM (0.02 mmol in 4 mL of CH₃NO₂) down to 10 μ M (0.04 μ mol in 4 mL of CH₃NO₂) for the online photoredox reaction while maintaining the concentrations of styrene 2 and Ru catalyst 4 the same as those in the experiments shown in Figure 2 (0.1 M styrene 2 and 100 μ M Ru 4). Indeed, when CPA 1 was diluted to 100 μ M, the product radical cation $3^{+\bullet}$ at m/z 237.1512 (Figure 3c;

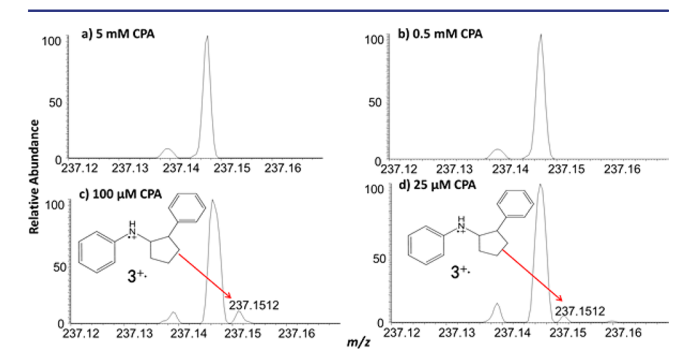


Figure 3. Zoomed-in ESI-MS spectra showing the influence of the CPA concentration on the observation of $3^{+\circ}$: (a) 5 mM CPA, (b) 0.5 mM CPA, (c) 100 μ M CPA, and (d) 25 μ M CPA. $3^{+\circ}$ was observed when the CPA concentration was decreased to 100 μ M. The absolute intensities for m/z 237.1512 in Figure 3c,d are 2.35 \times 10⁵ and 1.43 \times 10⁵ (arbitrary units), respectively. Note that no $1^{+\circ}$ was observed in these experiments, probably due to the presence of excess styrene (except for a small peak of $1^{+\circ}$ seen for the case of 5 mM CPA due to in-source oxidation). Also, no Ru(I) species was observed.

measured m/z, 237.1512; theoretical m/z, 237.1512; error, 0.0 ppm) was observed. The signal of $3^{+\bullet}$ appeared only when the laser pointer was turned on, supporting it being a photochemical product. Upon further dilution of CPA 1, the peak intensity of the CPA radical cation 3^{+•} decreased (Figure 3d). When the concentration of CPA 1 was decreased to 10 μ M, the peak at m/z 237 was not observed (data not shown), probably because the concentration of the resulting 3^{+•} was below the detection limit of our MS instrument. Notably, the observed 3^{+•} was not an artifact of the in-source ESI oxidation product. In a control experiment, ESI of the authentic product 3 did not give rise to an observable signal for 3^{+•}. Furthermore, direct irradiation of 3 in the presence of Ru catalyst 4 did not produce 3^{+•} either. These results not only showed the existence of the proposed product radical cation $3^{+\bullet}$ in the [3 + 2]annulation reaction but also verified our hypothesis that a low concentration of CPA 1 would favor the observation of 3+0.

To further confirm the assignment of observed $3^{+\bullet}$ and $[3 + H]^+$ ions, styrene 2 was replaced by styrene- α , β , and β - d_3 in the annulation reaction under otherwise identical conditions. The protonated final product- d_3 (3- d_3) at m/z 241 (measured m/z, 241.1778; theoretical m/z, 241.1779; error, -0.4 ppm) and the

product- d_3 radical cation (3- $d_3^{+\bullet}$) at m/z 240.1699 (Figure S5b, inset, measured m/z, 240.1699; theoretical m/z, 240.1700; error, -0.4 ppm) were both observed (Figure S5).

Chain Mechanism Investigation. Post-irradiation Chain Propagation. Encouraged by observing the dependence of detecting 3^{+•} on the concentration of CPA 1, we decided to investigate the chain propagation from a different angle: postirradiation. The original MS setup described in Figure 1a was modified to perform a sequential reaction experiment (Figure 1b). A mixing Tee was used to introduce CPA- d_5 1- d_5 into the silica capillary microreactor to further react with the irradiated reaction mixture of CPA 1. Ru(II) catalyst 4. and styrene 2. A degassed solution of CPA 1 (100 µM), [Ru(bpz)₃](PF₆)₂ 4 (100 μ M), and styrene 2 (0.1 M) was infused via channel 1 for irradiation. The degassed solution of CPA- d_5 1- d_5 (100 μ M) was infused via channel 2. The injection flow rate was 50 μ L/ min for both channels. This modified setup allowed the channel 1 reaction solution to be first irradiated by the blue laser pointer and then mixed with CPA- d_5 1- d_5 from channel 2 without light irradiation. If the chain process was involved, then radical cation intermediates 3^{+•} would induce CPA-d₅ to participate in the [3 + 2] annulation reaction to afford the annulation product- d_5 .

In a control study with no light irradiation (Figure 4a), m/z 134 and m/z 139 were observed, corresponding to protonated

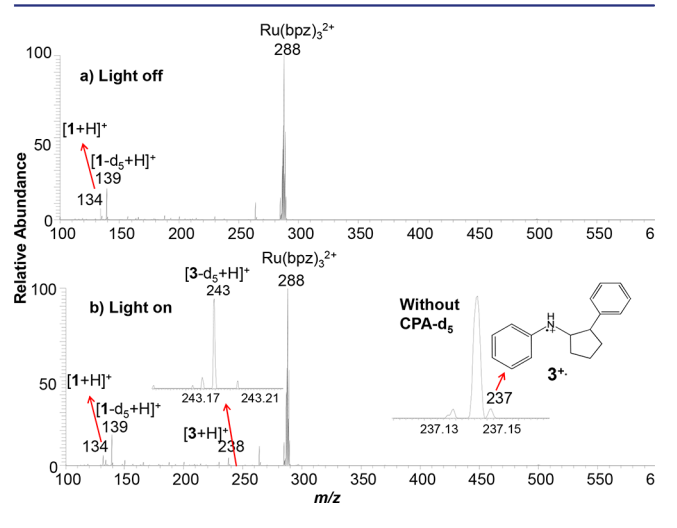


Figure 4. ESI-MS spectra of a post-irradiation reaction: a mixture of degassed CPA 1 (100 μ M), [Ru(bpz)₃](PF₆)₂ 4 (100 μ M), and styrene 2 (0.1 M) in CH₃NO₂ was first irradiated and then mixed with a degassed solution of CPA- d_5 (100 μ M) in CH₃NO₂ introduced via channel 2 (see apparatus in Figure 1b) for testing the chain reaction mechanism. (a) the light was turned off. (b) the light turned on. The inset shows a zoomed-in view of the ESI-MS spectrum from an irradiation experiment without adding CPA- d_5 .

CPA $[1 + H]^+$ and CPA- d_5 $[1 - d_5 + H]^+$, respectively. When the laser pointer was turned on for irradiation, the protonated [3 + 2] annulation product $[3 + H]^+$ peak at m/z 238 was clearly observed. More importantly, a new peak corresponding to the protonated [3 + 2] annulation product- d_5 $[3 - d_5 + H]^+$ at m/z 243 was also detected (measured m/z, 243.1900; theoretical m/z, 243.1904; error, 1.6 ppm; Figure 4b, inset). Moreover, before adding CPA- d_5 through channel 2 (only solvent was introduced via channel 2), the product radical cation $3^{+\bullet}$ at m/z 237 was observed (Figure 4b, inset). After mixing, the product radical cation $3^{+\bullet}$ disappeared. The consumption of the product radical cation $3^{+\bullet}$ with concurrent formation of the CPA product- d_5

provided another strong piece of evidence to support the chain propagation mechanism.

To rule out the possibility that the observed $[3-d_5 + H]^+$ resulted from the oxidation of CPA- d_5 by the pre-excited photocatalyst, a second control experiment was carried out in which a degassed solution of $[Ru(bpz)_3](PF_6)_2$ 4 (100 μ M) and styrene 2 (0.1 M) was infused via channel 1 for irradiation (CPA 1 was omitted) and the degassed solution of CPA- d_5 (100 μ M) was infused via channel 2. The injection flow rate for both channels was kept at 50 μ L/min. The protonated CPA- d_5 reaction product $[3-d_5 + H]^+$ at m/z 243 was not observed (Figure S6). Presumably because the lifetime of photoexcited 4 is much shorter than the transportation time for the reaction mixture to flow from the irradiation window to the Tee mixer (0.74 μ s vs about 472 ms), the photochemically pre-excited Ru catalyst 4 could be deactivated before reaching CPA- d_5 .

Oxidation of Substrate 1 by $3^{+\bullet}$. The remaining task in fully establishing the chain propagation process was to validate the oxidation of CPA 1 by the radical cation of the annulation product $3^{+\bullet}$ (Figure 5a). We initially attempted the generation

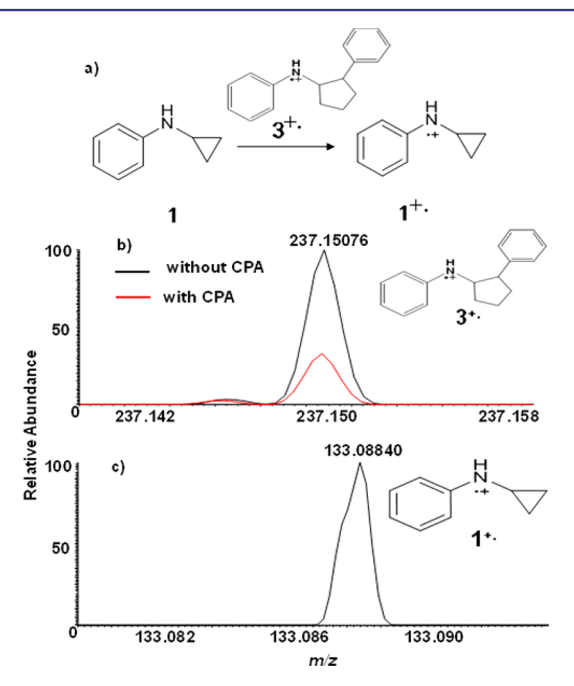


Figure 5. ESI-MS for monitoring of the oxidation of CPA 1 by 3^{+•}: a degassed solution of product 3 (1 mM) and LiOTf (1 mM) in ACN was infused into the electrochemical flow cell to generate 3^{+•}, which reacted with CPA 1 (introduced via channel 2). (a) Chemical equation showing the reaction between 3^{+•} and 1. (b) ESI-MS spectra (background subtracted) showing the formation of radical cation 3^{+•} when the oxidation potential was applied to the cell (black line, only solvent ACN was introduced via channel 2; red line, CPA 1 was introduced via channel 2). (c) ESI-MS spectrum (background subtracted) showing the formation of CPA radical cation 1^{+•} when the cell was turned on and CPA 1 was introduced in channel 2.

of 3^{+•} by photolysis of the authentic reaction product 3 in the presence of Ru catalyst 4. The targeted 3^{+•} was not observed, even though Stern–Volmer studies showed that product 3 was an effective quencher for photoexcited 4, albeit somewhat less effective than CPA 1 (Figures S14 and S15). We then attempted chemical oxidation of CPA 1 using a single-electron oxidant, tris(4-bromophenyl)ammoniumyl hexachloroantimonate. Although 3^{+•} was successfully generated, a large

amount of the oxidant remained. Because the unreactive oxidant could directly oxidize 1 and thus interfere with the targeted oxidation of 1 by $3^{+\bullet}$, we had to abandon this approach

Finally, we decided to focus on the generation of $3^{+\bullet}$ using electrochemical oxidation of 3. The setup described in Figure 1b was modified by adding a thin-layer electrochemical flow cell to perform the electrochemical oxidation (Figure 1c). A magic diamond electrode (12 × 30 mm) was used with LiOTf as the supporting electrolyte. The electrochemical flow cell was connected to a Tee mixer through which CPA 1 was introduced. A solution of the annulation product 3 (1 mM) and LiOTf (1 mM) in CH3CN was infused into the flow cell, and CH₃CN was first infused via channel 2. A potentiostat was used to apply potential for electro-oxidation. The injection flow rate for both channels was 10 μ L/min. When +3.0 V was applied to the flow cell to trigger the electrochemical oxidation of 3, the targeted radical cation 3^{+•} was observed (Figure 5b, black line). When the solvent, CH₃CN, was replaced by CPA 1 in CH₃CN (100 μ M) in channel 2, the signal of 3^{+•} decreased (Figure 5b, red line) with concomitant formation of the CPA radical cation 1^{+•} (Figure 5c). This set of data validated the oxidation of CPA 1 by the product radical cation 3^{+•}, which was also supported by our cyclic voltammetric measurements of 1 and 3 (Figure S8). Both have a very similar oxidation potential (ca. 0.8 V vs SCE).

To rule out the possibility that the observed CPA radical cation 1^{+•} was formed by reacting with other species in the oxidized solvent, a control experiment was performed in which only LiOTf (1 mM) in CH₃CN (without 3) was infused into the cell for oxidation under the same conditions and then mixed with CPA 1 (100 μ M). In this control experiment, no CPA radical cation 1^{+•} was generated (Figure S7), indicating that no other species from the electrochemical cell except 3⁺¹ could oxidize CPA 1.

Quantum Yield Measurement. To corroborate our MS studies on the elucidation of the chain mechanism, we measured the quantum yield of the [3 + 2] annulation of 3,5-dimethylcyclopropylaniline 5 and styrene 2. Using potassium ferrioxalate as an actinometer and a 300 W xenon lamp (50% light intensity, 439 ± 5 nm bandpass filter, high transmittance), we determined the quantum yield at time intervals of 15, 30, and 60 min (Figures S9-S12), 4g,i,6b and the quantum yield was calculated to be 1.64, 1.68, and 1.44, respectively, which stayed above 1 during the course of the experiment, supporting the chain mechanism. The low quantum yield on its own could lead to ambiguity in deciphering the chain mechanism^{4g} and therefore would require additional studies. However, our MS studies provided unequivocal evidence to support the chain mechanism.

On the basis of the low quantum yield we obtained for the [3] + 2] annulation, we anticipated that light/dark experiments might not reveal the chain mechanism. Not surprisingly, similar to Stephenson's, 6a Yoon's, 6b and others'4i,5 results, we observed that the annulation occurred only in the presence of light and stalled when the light source was off (Figure 6, details shown in the Supporting Information). Again, as with other reports, this result revealed the limitation of light/dark experiments to disprove the chain mechanism. The failure of light/dark experiments in distinguishing photoredox mechanisms from chain mechanisms is presumably due to the premise that most of the reactions under photoredox catalysis contain a short radical chain. Unfortunately, light/dark experiments do not

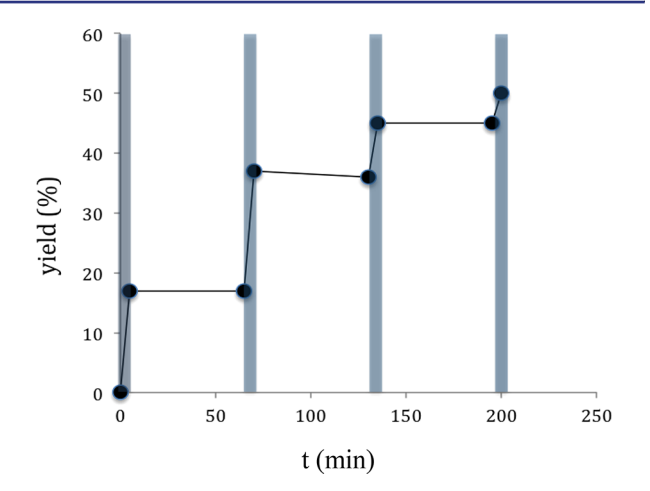


Figure 6. Light/dark experiments for the [3 + 2] annulation.

have a response fast enough to detect the radical chain. Our apparatus (Figure 1) not only possesses the inherently fast response of online ESI-MS methods but also enables coupling with an online photomicroreactor or an electrochemical cell to monitor post-irradiation reaction products (e.g., the [3 + 2]annulation product of CPA- d_5 in the dark, Figure 4b; oxidation of CPA 1 by electrochemically generated 3^{+•}, Figure 5). Both features make our apparatus a powerful tool to detect chain processes in photoredox reactions.

Photostability of Catalyst. Photostability is one of the key features of a good photocatalyst. However, because of the presence of various in situ generated radical species, deactivation of photocatalysts by adding one of these radical species to the catalyst's ligand is often encountered. 16 Recently, the Stephenson group delineated a deactivation pathway for Ir(ppy)₃ via ligand functionalization using a combination of kinetic, synthetic, and spectroscopic tools. 17 We were wondering whether we could use the online irradiation MS to study the potential deactivation pathway in the [3 + 2] annulation. This is particularly relevant to the catalyst used in the annulation reaction, $[Ru(bpz)_3](PF_6)_2$ 4, which has been shown to be less stable than other Ru complexes based on our observations. As shown in Figure 2b, in the absence of styrene 2, a new peak at m/z 354 was observed, which corresponds to the Ru complex monoalkylated by CPA. Upon CID (Figure S4), this ion dissociated into fragment ions $[CPA - H]^+$ (m/z 132), [354 - $CPA]^{2+}$ (m/z 288), $[354 - PhNHCH=CH₂]^{2+}$ (m/z 295), $[354 - PhNH_2]^{2+}$ (m/z 308), and $[Ru(bpz)_2 - H]^+$ (m/z 417), which indeed suggests that it is a covalently bonded adduct ion of CPA and the Ru catalyst. However, ligand shedding to the catalyst was not observed. In addition, to our surprise, in the presence of both CPA 1 and styrene 2, Ru complex 4 remained intact (Figure 2c). This interesting observation sheds light on the premise that a less robust photocatalyst such as Ru(bpz)₃](PF₆)₂ 4 could still be used as long as there are viable reactions to be catalyzed.

CONCLUSIONS

The recent surge of activity in visible-light photocatalysis has prompted organic chemists to study the mechanism of various reactions under photoredox catalysis. However, the mechanistic studies of these reactions have proven challenging, as there is lack of analytical tools that are capable of detecting transient intermediates in low quantity while also providing rich structural information. The ESI-MS setup with online

photolysis described herein, which requires a small amount of material (e.g., 400 nmol of both [Ru(bpz)₃](PF₆)₂ 4 and CPA 1) and possesses a fast response and high detection sensitivity, is a powerful tool to study visible-light photocatalysis mechanistically. The in situ ionization capability of ESI-MS with online irradiation allows us to detect key and short-lived species such as amine radical cations and Ru(bpz)₃⁺ and to examine the deactivation of photocatalysts. Moreover, by combining electrochemistry with MS, we are able to prove the viability of the oxidation of CPA 1 by $3^{+\bullet}$, generated by the electrochemical oxidation of 3. This result along with the postirradiation reaction study provides conclusive experimental support for the involvement of the chain mechanism in the [3 + 2] annulation reaction. Finally, this study provides another good example of using MS to detect elusive and transient reaction intermediates in low quantity.^{7,8} We believe that we have just scratched the surface of the potential of ESI-MS with online irradiation and online electrolysis to study visible-light photocatalysis, and more new applications are anticipated to come.

ASSOCIATED CONTENT

Supporting Information

The Supporting Information is available free of charge on the ACS Publications website at DOI: 10.1021/jacs.7b06319.

Experimental details, apparatus photos, and additional MS, MS/MS data, and quantum yield experimental results (PDF)

AUTHOR INFORMATION

Corresponding Authors

*nzheng@uark.edu

*chenh2@ohio.edu

ORCID

Nan Zheng: 0000-0002-0128-2877 Hao Chen: 0000-0001-8090-8593

Author Contributions

§Y.C., J.W., and Y.Z. contributed equally to this work.

Notes

The authors declare no competing financial interest.

ACKNOWLEDGMENTS

We thank Dr. Theresa H. Nguyen for early synthetic support and Professor Bill Durham for advice on quantum yield measurements. This work was supported by an NSF Career Award (CHE-1255539) and the National Institutes of Health under grant number P30 GM103450 from the National Institute of General Medical Sciences to N.Z., as well as NSF IDBR (CHE-1455554), NSF (CHE-1709075), and NSF MRI (CHE-1428787) to H.C. Y.C. thanks the Ohio Third Frontier Fund for a research assistantship.

REFERENCES

(1) (a) Prier, C. K.; Rankic, D. A.; MacMillan, D. W. C. Chem. Rev. 2013, 113, 5322-5363. (b) Xuan, J.; Xiao, W.-J. Angew. Chem., Int. Ed. 2012, 51, 6828-6838. (c) Fukuzumi, S.; Ohkubo, K. Chem. Sci. 2013, 4, 561-574. (d) Yoon, T. P. ACS Catal. 2013, 3, 895-902. (e) Romero, N. A.; Nicewicz, D. A. Chem. Rev. 2016, 116, 10075-10166.

(2) (a) Gentry, E. C.; Knowles, R. R. Acc. Chem. Res. 2016, 49, 1546-1556. (b) Ghosh, I.; Marzo, L.; Das, A.; Shaikh, R.; König, B. Acc. Chem. Res. 2016, 49, 1566-1577. (c) Staveness, D.; Bosque, I.; Stephenson, C. R. J. Acc. Chem. Res. 2016, 49, 2295-2306. (d) Goddard, J.-P.; Ollivier, C.; Fensterbank, L. Acc. Chem. Res. 2016, 49, 1924-1936. (e) Nakajima, K.; Miyake, Y.; Nishibayashi, Y. Acc. Chem. Res. 2016, 49, 1946-1956. (f) Chen, J.-R.; Hu, X.-Q.; Lu, L.-Q.; Xiao, W.-J. Chem. Soc. Rev. 2016, 45, 2044-2056.

(3) (a) Ye, Y.; Sanford, M. S. J. Am. Chem. Soc. 2012, 134, 9034-9037. (b) DiRocco, D. A.; Rovis, T. J. Am. Chem. Soc. 2012, 134, 8094-8097. (c) Sahoo, B.; Hopkinson, M. N.; Glorius, F. J. Am. Chem. Soc. 2013, 135, 5505-5508. (d) Zoller, J.; Fabry, D. C.; Ronge, M. A.; Rueping, M. Angew. Chem., Int. Ed. 2014, 53, 13264-13268. (e) Tellis, J. C.; Primer, D. N.; Molander, G. A. Science 2014, 345, 433-436. (f) Zuo, Z.; Ahneman, D. T.; Chu, L.; Terrett, J. A.; Doyle, A. G.; MacMillan, D. W. C. Science 2014, 345, 437-440. (g) Du, J.; Skubi, K. L.; Schultz, D. M.; Yoon, T. P. Science 2014, 344, 392-396. (h) Xuan, J.; Zeng, T.-T.; Feng, Z.-J.; Deng, Q.-H.; Chen, J.-R.; Lu, L.-Q.; Xiao, W.-J.; Alper, H. Angew. Chem., Int. Ed. 2015, 54, 1625-1628. (i) Jeffrey, J. L.; Terrett, J. A.; MacMillan, D. W. C. Science 2015, 349, 1532–1536. (j) Terrett, J. A.; Cuthbertson, J. D.; Shurtleff, V. W.; MacMillan, D. W. C. Nature 2015, 524, 330-334. (k) Uraguchi, D.; Kinoshita, N.; Kizu, T.; Ooi, T. J. Am. Chem. Soc. 2015, 137, 13768-13771. (l) Kainz, Q. M.; Matier, C. D.; Bartoszewicz, A.; Zultanski, S. L.; Peters, J. C.; Fu, G. C. Science 2016, 351, 681-684. (m) Corcoran, E. B.; Pirnot, M. T.; Lin, S.; Dreher, D. A.; DiRocco, D. A.; Davies, I. A.; Buchwald, S. L.; MacMillan, D. W. C. Science 2016, 353, 279-283. (4) For selected examples, see (a) Kayser, R. H.; Young, R. H. Photochem. Photobiol. 1976, 24, 395-401. (b) Delaive, P. J.; Foreman, T. K.; Giannotti, C.; Whitten, D. G. J. Am. Chem. Soc. 1980, 102, 5627-5631. (c) Andrews, R. S.; Becker, J. J.; Gagne, M. R. Org. Lett. 2011, 13, 2406-2409. (d) Liu, Q.; Li, Y.-N.; Zhang, H.-H.; Chen, B.; Tung, C.-H.; Wu, L.-Z. Chem. - Eur. J. 2012, 18, 620-627. (e) Pitre, S. P.; McTiernan, C. D.; Ismaili, H.; Scaiano, J. C. J. Am. Chem. Soc. 2013, 135, 13286-13289. (f) Romero, N. A.; Nicewicz, D. A. J. Am. Chem. Soc. 2014, 136, 17024-17035. (g) Yayla, H. G.; Peng, F.; Mangion, I. K.; McLaughlin, M.; Campeau, L.-C.; Davies, I. W.; DiRocco, D. A.; Knowles, R. R. Chem. Sci. 2016, 7, 2066-2073. (h) Meyer, A. U.; Straková, K.; Slanina, T.; König, B. Chem. - Eur. J. 2016, 22, 8694-8699. (i) Shen, X.; Harms, K.; Marsch, M.; Meggers, E. Chem. - Eur. J. 2016, 22, 9102-9105. (j) Bartling, H.; Eisenhofer, A.; König, B.; Gschwind, R. W. J. Am. Chem. Soc. 2016, 138, 11860-11871. (k) Pitre, S. P.; McTiernan, C. D.; Scaiano, J. C. Acc. Chem. Res. 2016, 49, 1320-1330. (1) Neumann, M.; Fuldner, S.; Konig, B.; Zeitler, K. Angew. Chem., Int. Ed. 2011, 50, 951-954. (m) Nappi, M.; Bergonzini, G.; Melchiorre, P. Angew. Chem., Int. Ed. 2014, 53, 4921-4925.

(5) (a) Miyake, Y.; Nakajima, K.; Nishibayashi, Y. J. Am. Chem. Soc. 2012, 134, 3338-3341. (b) Jiang, H.; Cheng, Y.; Wang, R.; Zheng, M.; Zhang, Y.; Yu, S. Angew. Chem., Int. Ed. 2013, 52, 13289-13292. (c) Zou, Y.-Q.; Guo, W.; Liu, F.-L.; Lu, L.-Q.; Chen, J.-R.; Xiao, W.-J. Green Chem. 2014, 16, 3787-3795. (d) Lu, P.; Hou, T.; Gu, X.; Li, P. Org. Lett. 2015, 17, 1954-1957.

(6) (a) Wallentin, C.-J.; Nguyen, J. D.; Finkbeiner, P.; Stephenson, C. R. J. J. Am. Chem. Soc. 2012, 134, 8875-8884. (b) Cismesia, M. A.; Yoon, T. P. Chem. Sci. 2015, 6, 5426-5434.

(7) (a) Wilson, S. R.; Perez, J.; Pasternak, A. J. Am. Chem. Soc. 1993, 115, 1994-1997. (b) Arakawa, R.; Lu, J.; Yoshimura, A.; Nozaki, K.; Ohno, T.; Doe, H.; Matsuo, T. Inorg. Chem. 1995, 34, 3874-8. (c) Sam, J. W.; Tang, X.-J.; Magliozzo, R. S.; Peisach. J. Am. Chem. Soc. 1995, 117, 1012-1018. (d) Feichtinger, D.; Plattner, D. A. Angew. Chem., Int. Ed. Engl. 1997, 36, 1718-1719. (e) Feichtinger, D.; Plattner, D. A.; Chen, P. J. Am. Chem. Soc. 1998, 120, 7125-7126. (f) Ding, W.; Johnson, K. A.; Amster, I. J.; Kutal, C. Inorg. Chem. 2001, 40, 6865-6866. (g) Julian, R. R.; May, J. A.; Stoltz, B. M.; Beauchamp, J. L. J. Am. Chem. Soc. 2003, 125, 4478-4486. (h) Meyer, S.; Koch, R.; Metzger, J. O. Angew. Chem., Int. Ed. 2003, 42, 4700-4703. (i) Wilson, D. J.; Konermann, L. Anal. Chem. 2003, 75, 6408-6414. (j) Sabino, A. A.; Machado, A. H. L.; Correia, C. R. D.; Eberlin, M. N. Angew. Chem., Int. Ed. 2004, 43, 2514-2518. (k) Chen, P. Angew. Chem., Int. Ed. 2003, 42, 2832-2847. (1) Fuermeier, S.; Griep-Raming, J.; Hayen, A.; Metzger, J. O. Chem. - Eur. J. 2005, 11, 5545-5554. (m) Bao, H.; Zhou, J.; Wang, Z.; Guo, Y.; You, T.; Ding, K. J. Am. Chem. Soc. 2008,

- 130, 10116–10127. (n) Meyer, M. M.; Khairallah, G. N.; Kass, S. R.; O'Hair, R. A. J. Angew. Chem., Int. Ed. 2009, 48, 2934–2936. (o) Yunker, L. P. E.; Stoddard, R. L.; McIndoe, J. S. J. Mass Spectrom. 2014, 49, 1–8. (p) Iacobucci, C.; Reale, S.; De Angelis, F. Angew. Chem., Int. Ed. 2016, 55, 2980–2993. (q) Chen, S.; Wan, Q.; Badu-Tawiah, A. K. Angew. Chem., Int. Ed. 2016, 55, 9345–9349. (r) Widjaja, F.; Jin, Z.; Nash, J. J.; Kenttämaa, H. I. J. Am. Chem. Soc. 2012, 134, 2085–2093. (s) Fürmeier, S.; Metzger, J. O. J. Am. Chem. Soc. 2004, 126, 14485–14492.
- (8) (a) Takáts, Z.; Wiseman, J. M.; Gologan, B.; Cooks, R. G. Science 2004, 306, 471–473. (b) Perry, R. H.; Splendore, M.; Chien, A.; Davis, N. K.; Zare, R. N. Angew. Chem., Int. Ed. 2011, 50, 250–254. (c) Perry, R. H.; Brownell, K. R.; Chingin, K.; Cahill, T. J., III; Waymouth, R. M.; Zare, R. N. Proc. Natl. Acad. Sci. U. S. A. 2012, 109, 2246–2250. (d) Brown, T. A.; Chen, H.; Zare, R. N. J. Am. Chem. Soc. 2015, 137, 7274–7277. (e) Zheng, Q.; Liu, Y.; Chen, Q.; Hu, M.; Helmy, R.; Sherer, E. C.; Welch, C. J.; Chen, H. J. Am. Chem. Soc. 2015, 137, 14035–14038.
- (9) Maity, S.; Zhu, M.; Shinabery, R. S.; Zheng, N. Angew. Chem., Int. Ed. 2012, 51, 222–226.
- (10) (a) Nguyen, T. H.; Maity, S.; Zheng, N. Beilstein J. Org. Chem. **2014**, 10, 975–980. (b) Nguyen, T. H.; Morris, S. A.; Zheng, N. Adv. Synth. Catal. **2014**, 356, 2831–2837.
- (11) Rassadin, V. A.; Six, Y. Tetrahedron 2016, 72, 4701-4757.
- (12) (a) Qin, X.-Z.; Williams, F. J. J. Am. Chem. Soc. 1987, 109, 595—597. (b) Li, X.; Grimm, M. L.; Igarashi, K.; Castagnoli, N., Jr.; Tanko, J. M. Chem. Commun. 2007, 2648—2650.
- (13) (a) Keizer, S. P.; Han, W.; Stillman, M. J. *Inorg. Chem.* **2002**, *41*, 353–358. (b) Ma, X.; Zhao, X.; Li, J.; Zhang, W.; Cheng, J.-X.; Ouyang, Z.; Xia, Y. *Anal. Chem.* **2016**, *88*, 8931–8935.
- (14) (a) Brown, T. A.; Chen, H.; Zare, R. N. Angew. Chem, Int. Ed. 2015, 54, 11183–11185. (c) Brown, T. A.; Hosseini-Nassab, N.; Chen, H.; Zare, R. N. Chem. Sci. 2016, 7, 329–332. (d) Zheng, Q.; Chen, H. Annu. Rev. Anal. Chem. 2016, 9 (1), 411–448. (e) Zhang, Y.; Yuan, Z.; Dewald, H. D.; Chen, H. Chem. Commun. 2011, 47, 4171–4173. (f) Zheng, Q.; Zhang, H.; Tong, L.; Wu, S.; Chen, H. Anal. Chem. 2014, 86, 8983–8991. (g) Li, J.; Dewald, H. D.; Chen, H. Anal. Chem. 2009, 81, 9716–9722.
- (15) Van Berkel, G. J.; McLuckey, S. A.; Glish, G. L. Anal. Chem. 1992, 64, 1586-1593.
- (16) Schmidbauer, S.; Hohenleutner, A.; König, B. Beilstein J. Org. Chem. 2013, 9, 2088–2096.
- (17) Devery, J. J., III; Douglas, J. J.; Nguyen, J. D.; Cole, K. P.; Flowers, R. A., II; Stephenson, C. R. J. Chem. Sci. 2015, 6, 537–541.